Original Article

Mebendazole induces apoptosis and inhibits migration via the reactive oxygen species-mediated STAT3 signaling downregulation in non-small cell lung cancer

Zhipan Liang[1#], Qiuyun Chen[2#], Liuying Pan[1], Xiaowei She[1], Tengfei Chen[1]

[1]Department of Thoracic Surgery, The Affiliated Suzhou Hospital of Nanjing Medical University, Suzhou Municipal Hospital, Gusu School, Nanjing Medical University, Suzhou, China; [2]Department of Clinical Nursing, Dushu Lake Hospital Affiliated to Soochow University, Suzhou, China

Contributions: (I) Conception and design: T Chen; (II) Administrative support: T Chen, X She; (III) Provision of study materials or patients: Z Liang, Q Chen, L Pan; (IV) Collection and assembly of data: Z Liang, Q Chen; (V) Data analysis and interpretation: Z Liang, T Chen; (VI) Manuscript writing: All authors; (VII) Final approval of manuscript: All authors.

[#]These authors contributed equally to this work.

Correspondence to: Tengfei Chen, PhD; Xiaowei She, MD. Department of Thoracic Surgery, The Affiliated Suzhou Hospital of Nanjing Medical University, Suzhou Municipal Hospital, Gusu School, Nanjing Medical University, No. 458 Shizi Street, Gusu District, Suzhou 215031, China. Email: tengfeicheny@126.com; drshxw@163.com.

Background: The incidence and mortality of non-small cell lung cancer (NSCLC) are extremely high. Previous research has confirmed that the signal transducer and activator of the transcription 3 (STAT3) protein critically participate in the tumorigenesis of NSCLC. Mebendazole (MBZ) has exerts a larger number of pharmacological activities and has anticancer effects in lung cancer, but its mechanism of action remains unclear. This study thus aimed to clarify the impacts of MBZ on NSCLC cell.

Methods: Cell proliferation, migration, and apoptosis were investigated via cell counting kit 8 (CCK-8) assay, Transwell assay, colony formation assay, wound-healing assay, and flow cytometry. Reactive oxygen species (ROS) were detected with a multifunctional microplate reader. Markers of cell migration and apoptosis were detected with Western blotting. The transcriptional activity of STAT3 was detected via luciferase assay. ROS scavenger N-acetylcysteine (NAC) was used to determine the effect of MBZ on NSCLC via ROS-regulated STAT3 inactivation and apoptosis. A xenograft model was constructed *in vivo* to investigate the role of MBZ in NSCLC tumor growth.

Results: The findings demonstrated that MBZ inhibited NSCLC cell proliferation and migration while promoting apoptosis through triggering ROS generation. In addition, the Janus kinase 2 (JAK2)-STAT3 signaling pathway was abrogated with the treatment of MBZ. NAC could distinctly weaken MBZ-induced apoptosis and STAT3 inactivation. Moreover, MBZ inhibited the tumor growth of NSCLC *in vivo*.

Conclusions: In summary, MBZ inhibited NSCLC cell viability and migration by inducing cell apoptosis via the ROS-JAK2-STAT3 signaling pathway. These data provide a theoretical basis for the use of MBZ in treating NSCLC.

Keywords: Non-small cell lung cancer (NSCLC); mebendazole (MBZ); signal transducer and activator of the transcription 3 (STAT3); reactive oxygen species (ROS)

Submitted Dec 29, 2023. Accepted for publication Feb 04, 2024. Published online Feb 27, 2024.
doi: 10.21037/jtd-23-1978
View this article at: https://dx.doi.org/10.21037/jtd-23-1978

Introduction

Lung cancer is the leading cause of cancer-related deaths (1). Non-small cell lung cancer (NSCLC), which accounts for an estimated 85% of lung cancer cases, is often resistant to radiation and chemotherapy (2,3). Since contemporary treatment modalities are insufficient, novel cures are essential to reduce the results of the growing incidence in NSCLC.

The signal transducer and activator of transcription 3 (STAT3) performs an essential role in tumor progression and mediates many cell processes, including proliferation and apoptosis (4,5). STAT3 was first identified as an oncogene required for epithelial cell transformation (6). The STAT3 pathway is frequently overactive in NSCLC, and STAT3 expression correlates with poor survival, making it a promising target for the design of novel cancer drugs (7). In addition, reactive oxygen species (ROS) act as critical intracellular messengers in cell proliferation, differentiation, and survival (8). Furthermore, related studies have confirmed that upregulation of ROS could suppress tumor growth by abrogating the Janus kinase 2 (JAK2)-STAT3 signaling pathway in several tumors, including hepatocellular carcinoma (9), multiple myeloma (10), and ovarian cancer (11). Consequently, ROS has been targeted by numerous anticancer drugs. For example, isoorientin can suppress the growth of lung cancer cells via the ROS-regulated STAT3 signaling cascade (12).

Mebendazole (methyl 5-benzoyl-2-benzimidazole-carbamate) (MBZ) has been used to treat helminthic diseases as an anthelmintic drug. In addition, MBZ exerts anticancer activities, such as microtubule polymerization arrest, cell apoptosis, cell cycle arrest, antiangiogenesis, and blockage of glucose transport (13,14). Previous studies have shown that MBZ possesses antitumor properties by triggering apoptosis and cell cycle arrest in NSCLC cells (15,16). However, the mechanism by which MBZ induces NSCLC cell apoptosis is still unknown. Furthermore, MBZ can inhibit the expression of phosphorylated AKT and STAT3 to suppress the metastatic potential of cells of advanced thyroid cancer (17). Therefore, analyzing MBZ to determine its therapeutic potential for NSCLC via the inactivation of the STAT3 pathway may be fruitful. In this study, human NSCLC cell lines, H460 and A549, were employed to examine the effect of MBZ on cell growth repression and apoptosis, as well as the related mechanism. We present this article in accordance with the ARRIVE and MDAR reporting checklists (available at https://jtd.amegroups.com/article/view/10.21037/jtd-23-1978/rc).

Highlight box

Key findings

- This study revealed that mebendazole (MBZ)-induced reactive oxygen species (ROS) accumulation inhibits the activation of Janus kinase 2 (JAK2)-signal transducer and activator of transcription 3 (STAT3) signaling pathway, resulting in non-small cell lung cancer (NSCLC) cell apoptosis and migration inhibition.

What is known and what is new?

- MBZ exerts a larger number of pharmacological activities and has anticancer effects in lung cancer.
- MBZ triggers ROS generation and inhibits NSCLC cell proliferation and migration while promoting apoptosis via ROS-JAK2-STAT3 signaling pathway.

What is the implication, and what should change now?

- It may be feasible for MBZ to treat NSCLC through ROS-JAK2-STAT3 signaling pathway. The mechanism by which MBZ enhances ROS requires further investigation.

Methods

Cell lines and cell culture

The A549 and H460 human cancer cell lines were purchased from the American Type Collection (ATCC, Manassas, VI, USA). These cells were grown in the Dulbecco's modified Eagle's medium (DMEM; Gibco, Thermo Fisher Scientific, Waltham, MA, USA). Cells were enriched with 10% heat-inactivated fetal bovine serum (FBS; Gibco, Thermo Fisher Scientific, Inc.) and 1% penicillin and streptomycin, and then cultured at 37 ℃ in a 5% CO_2 atmosphere.

Reagents and antibodies

MBZ was purchased from MedChemExpress (Monmouth Junction, NJ, USA). N-acetylcysteine (NAC) was purchased from Sigma-Aldrich (St. Louis, MI, USA). Stattic was purchased from Selleck. β-actin (#3700), β-tubulin (#2128), E-Cadherin (#14472), N-Cadherin (#13116), ADP-ribose polymerase (PARP; #9532), JAK2 (#3230), caspase 3 (#9662), STAT3 (#9139), cleaved caspase 3 (#9661), C-MYC (#18583), phosphorylated JAK2 (p-JAK2) (#66245), Bcl-xl (#2764), SNAI1 (#3879), TWIST1 (#69366), and phosphorylated STAT3 (Tyr705) (p-STAT3) (#9145) antibodies were acquired from Cell Signaling Technology (Danvers, MA, USA).

Cell viability and colony formation assay

Cell proliferation of MBZ treatment on A549 and H460 cells was investigated with cell counting kit-8 (CCK-8) assay. Cells were seeded at concentrations of 1×10^4 cells/well into 96-dish culture plates, which was followed by incubation at 37 ℃ for 24 h. Cells were then treated with a variety of MBZ titrations (0, 0.001, 0.01, 0.1, 0.5, 1, and 10 μM) for 24, 48, and 72 h. Subsequently, a microplate reader (Agilent Technologies, Inc., Santa Clara, CA, USA) was employed to read the absorbencies of the cells at 450 nm. Finally, the obtained optical density (OD) values were analyzed, and the respective half maximal inhibitory concentration (IC_{50}) values were then acquired via GraphPad Prism software (GraphPad Software, Inc., San Diego, CA, USA).

In the colony formation assays, seeding of 500 cells/well was performed in 6-well culture dishes, and cells were grown using the DMEM growth medium enriched with 10% FBS. MBZ was added into each well for approximately 14 days until the cells grew into visible colonies. Subsequently, 4% paraformaldehyde was employed to perform colony fixation, which was followed by staining for 20 min using 0.1% crystal violet at room temperature. The crystal violet-stained colonies were photographed. A collection of 40 or more cells is counted as a single colony. Each test was repeated three times.

Wound-healing analysis

A549 and H460 cells were planted into 6-well culture plates at a concentration of 5×10^5 cells per well and grown for 24 h until the degree of fusion was 90%. Thereafter, cells were treated with serum-free medium for 24 h, and then the monolayers were scraped for confluent cells using a 1,000-μL sterile pipette tip to yield a wound in each well. After the scraped surface was washed with phosphate-buffered saline (PBS) three times to remove the floating cells, photographing of the wounded monolayers was completed using a microscope. Cells were then incubated in the absence or presence of MBZ (0.1 μM) for 24 h. Cells that had migrated into the wound region were photographed, and the mean distance of migrating cells was evaluated using a phase-contrast microscope (×40).

Transwell migration assay

To analyze cell migration, the cancer cells (1×10^5) were seeded into the upper chamber of Transwell inserts with 8-μm pores (Corning, NY, USA). The cells were grown in 0.1% FBS mixed with MBZ. Following this, 600 μL of complete medium enriched with 20% FBS was introduced to the lower chambers. Thereafter, we allowed the cells to migrate for 24 h. A cotton wool was used to swab the upper surfaces of the chambers, and then the migrated cells were fixed with 4% paraformaldehyde. Subsequently, 0.1% crystal violet staining was performed, and the invading cells in five randomly selected microscope fields were counted (×200).

Western blot analysis

Lysing of the samples was performed for 30 min using ice-chilled radioimmunoprecipitation assay (RIPA) buffer and protease inhibitor (Thermo Fisher Scientific). Centrifugation of the lysates was carried out, and then the supernatant aliquoted to fresh microfuge tubes. A bicinchoninic acid (BCA) protein assay kit (Thermo Fisher Scientific) was employed to assay the protein concentration. Thereafter, equal volumes of the proteins were fractionated on a sodium dodecyl sulfate–polyacrylamide gel electrophoresis (SDS-PAGE) gel, and the resolved proteins were transfer-embedded onto polyvinylidene fluoride (PVDF) membranes (MilliporeSigma, Burlington, MA, USA). Blocking of the membranes at room temperature for 1 h was accomplished using 5% skimmed milk. Subsequently, overnight incubation with corresponding primary antibodies was conducted at 4 ℃, which was followed by three washes with tris-buffered saline with Tween20 (TBST). Subsequently, the membranes were conjugated with the respective secondary antibodies for 1 h via incubation. Following 3 washes with TBST, an enhanced chemiluminescence kit (MilliporeSigma) was used to detect the signals.

Cell apoptosis assessment

Cells were planted in 6-well culture dishes at a titer of 1×10^5/well and then treated with 20 μM of MBZ or 10 mM of NAC for 72 h. The cells were then collected, rinsed twice using cold PBS, and resuspended in binding buffer-added Annexin V-fluorescein isothiocyanate (FITC) and propidium iodide (PI; MultiSciences Biotech Co., Ltd., Hangzhou, China). The apoptosis tests were carried using an Accuri C6 (BD Biosciences, Franklin Lakes, NJ, USA). ModFit LT software (FACSCalibur, BD Biosciences) was

employed in data analysis.

Intracellular ROS production analysis

Production of the intracellular ROS was assayed using a Reactive Oxygen Species Assay Kit (Beyotime, Haimen, China). Cells were seeded in 6-well dish culture dishes overnight and then treated with MBZ (0.5 μM) for 72 h. Subsequently, the cells were collected, and incubation with 10 μM of DCFH-DA (diacetyldichlorofluorescein) was conducted in the dark for 30 min. The cells were rinsed three times, the ROS contents were assayed on a multifunctional microplate reader (Flex Station 3, San Jose, CA, USA), and then the cells were collected. The protein titers were assayed using a Pierce BCA protein assay kit (Thermo Fisher Scientific).

Transient transfection and luciferase assay

A549 and H460 cells were cotransfected with pSTAT3 Luci and β-galactosidase (β-gal) plasmids (pGL4; Promega, Madison, WI, USA). The transfection was performed in 24-well dish plates, and 24 h later, the cells were exposed to NAC in the presence or absence of MBZ for 72 h. Luciferase enzyme activity and β-gal activity were determined as outlined in the manufacturer-provided protocol (Promega). The relative luciferase activity was normalized to the β-gal activity and calculated as an average of three independent experiments.

In vivo tumor model

Male, 3- to 5-week-old BALB/c nude mice were purchased from Shanghai Laboratory Animal Center (Shanghai, China). A549 cells were digested and washed with PBS three times. Subsequently, 5×10^7/mL cells were collected and mixed with Matrigel (Corning) at a 1:1 ratio by volume. A 100-μL volume of cell suspension was injected subcutaneously into the back region of mice. One week after cell implantation, the mice were randomly divided into two groups: one group received vehicle as the control, and the other group were orally administered MBZ (50 mg/kg) every other day for 3 weeks (five mice in each group). The tumor size and mice body were recorded every other day and calculated according to the following formula: tumor size (mm^3) = (length × $width^2$) × 0.5. A protocol was prepared before the study without registration. Animal experiments were performed under a project license (No. 202008A629) granted by ethics board of Soochow University, in compliance with institutional guidelines for the care and use of animals.

Statistical analysis

All data are expressed as the mean ± standard deviation (SD). The difference between two groups was determined using a two-tailed unpaired *t*-test. Differences among three or more groups were determined using one-way analysis of variance (ANOVA).

Results

MBZ suppressed proliferation and colony formation of NSCLC cells

The influences of MBZ on the proliferation of NSCLC cells were explored using the CCK-8 kits. As a result, MBZ suppressed the proliferation of A549 and H460 cells in a time-dependent and concentration-dependent manner (*Figure 1A*,*1B*). After incubation with MBZ for 48 h, the A549 IC_{50} values were 0.4001±0.0521 μM, and the H460 cell IC_{50} values were 0.2608±0.0388 μM (*Figure 1A*,*1B*). Next, we examined the suppressive influences of lower doses of MBZ (0.1 μM) on the colony formation of NSCLC cells. After 14 days of continuous culture, MBZ also diminished the colony formation of A549 and H460 cells (*Figure 1C*). These data suggested that MBZ had promising anti-NSCLC properties.

MBZ suppressed NSCLC cell migration

To evaluate the ability of MBZ to suppress the migration of A549 and H460 cells, Transwell migration and wound-healing assays were conducted. The cells treated with 0 μM of MBZ exhibited a comparatively high rate of wound closure (*Figure 2A*) and migration through Transwell membranes (*Figure 2B*). Moreover, some epithelial-to-mesenchymal transition (EMT)-correlated biosignatures were identified via Western blotting. Thus, after A549 and H460 cells were treated with MBZ, the mesenchymal biomarker N-cadherin was diminished and the epithelial biosignature E-cadherin was elevated (*Figure 2C*). Therefore, MBZ may suppress the cell migration of NSCLC cells by inhibiting EMT.

MBZ induced apoptosis through ROS accumulation in NSCLC cells

As MBZ inhibited A549 and H460 proliferation and

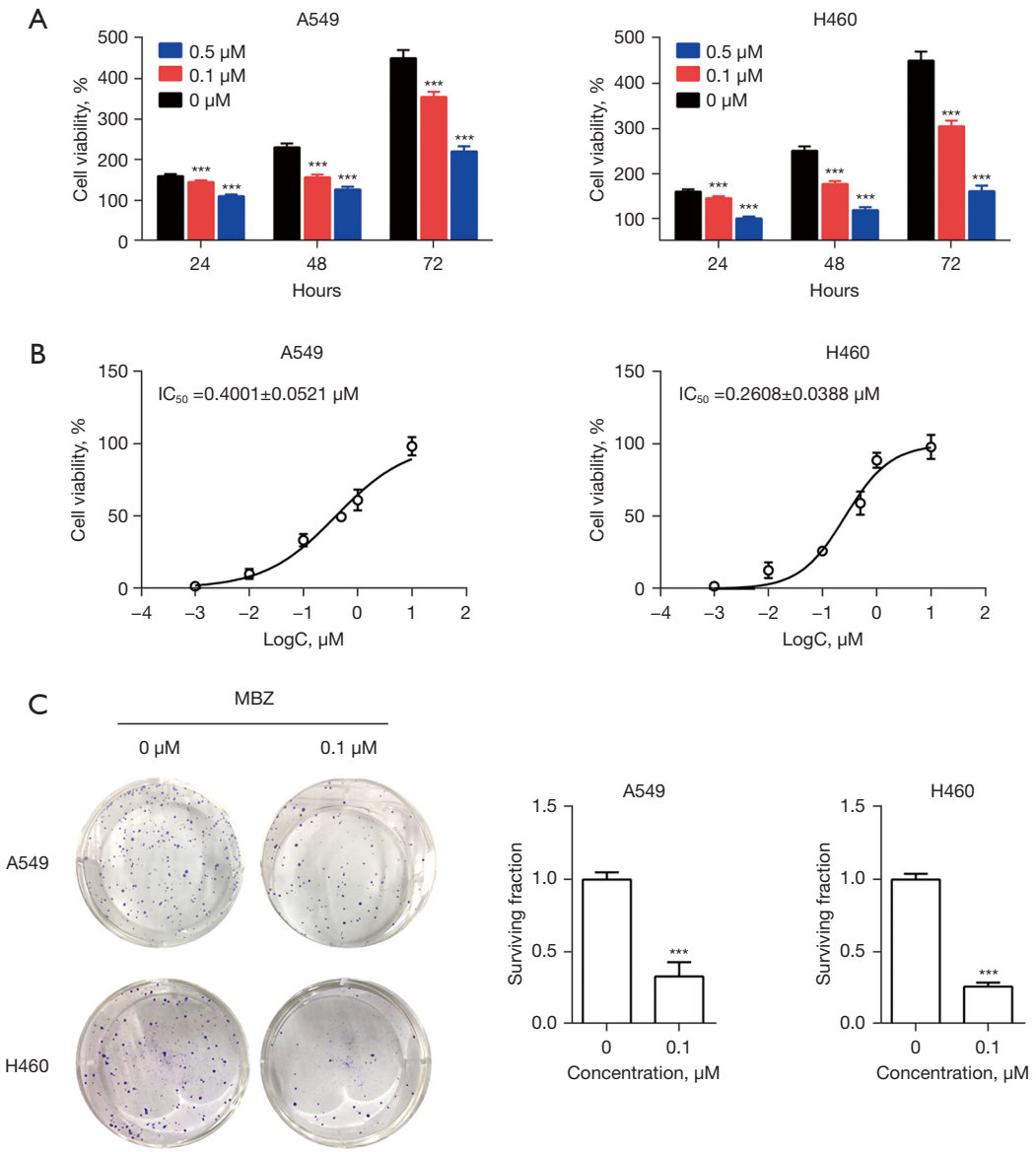

Figure 1 MBZ inhibited A549 and H460 proliferation. (A) A549 and H460 cells were administered with MBZ at titers of 0, 0.1, and 0.5 μM. At 24, 48 and 72 h, CCK-8 assay was carried out, and cell viability was assayed. Data from three independent assays were pooled. (B) A549 and H460 cells were administered with MBZ at titers of 0, 0.001, 0.01, 0.1, 0.5, 1, and 10 μM. At 48 h, CCK-8 assay was carried out, and cell viability was assayed. Data from three independent assays were pooled. (C) A549 and H460 cells were administered MBZ (0.1 μM) for about 14 days. Colonies were stained using crystal violet. The calculation was performed to determine the percentage of colony formation, relative to the values observed in untreated control cells. Data from three independent assays were pooled. ***, P<0.001. IC_{50}, half maximal inhibitory concentration; MBZ, mebendazole; CCK-8, cell counting kit 8.

migration, MBZ may significantly trigger apoptosis on these cells. Therefore, we next explored the influence of MBZ on NSCLC cell apoptosis. Annexin V-FITC and PI staining assay showed that MBZ triggered NSCLC cell apoptosis (*Figure 3A*). In addition, apoptosis markers, including PARP and cleaved caspase-3, were induced by MBZ (*Figure 3B*), suggesting that MBZ might promote apoptosis in NSCLC cells.

Since ROS are pivotal modulators in apoptosis (18), we next applied assays to determine if the elevated apoptosis

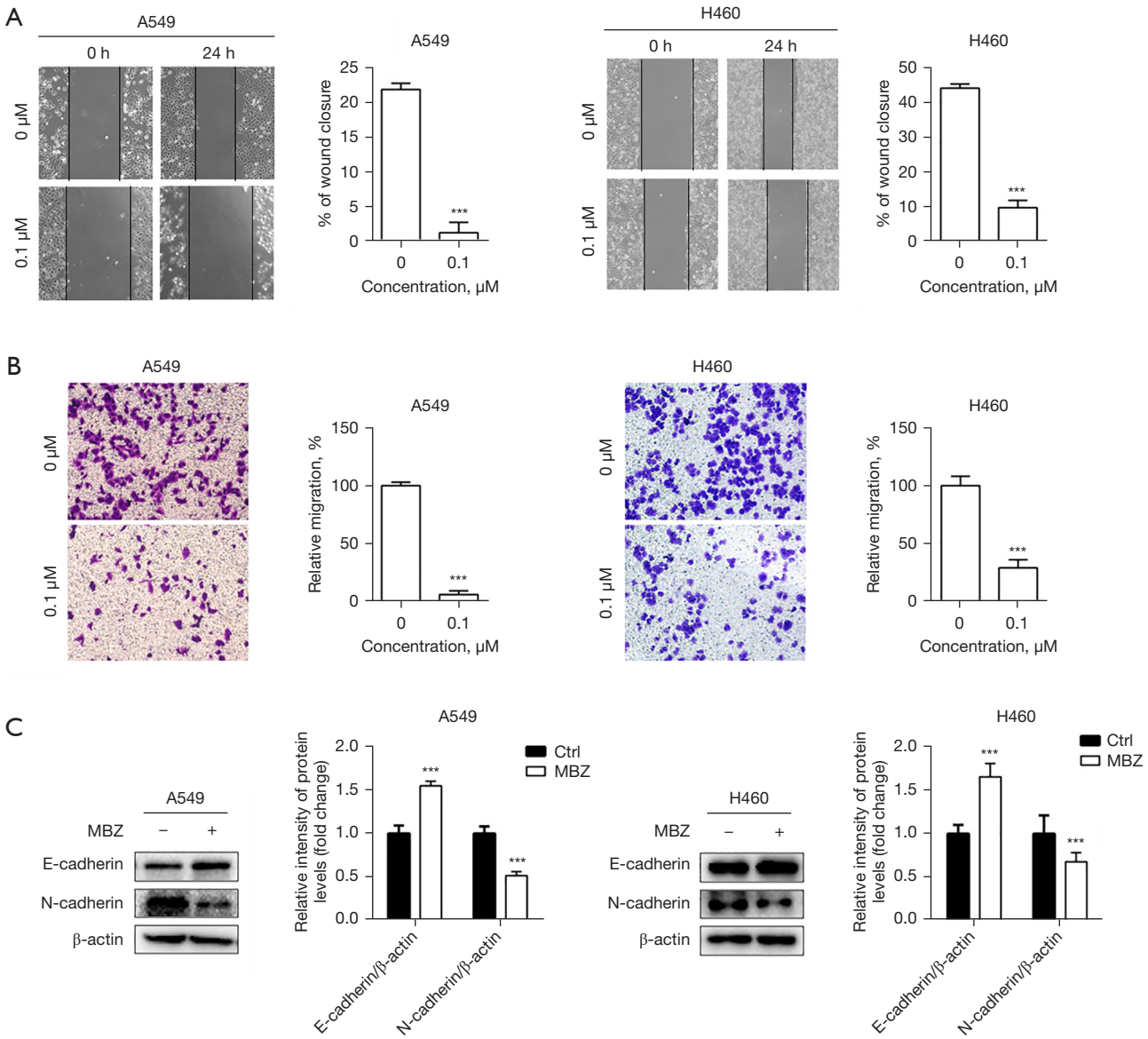

Figure 2 MBZ inhibited A549 and H460 cell migration. (A) Images and wound quantification of A549 and H460 cells administered MBZ (0.1 μM) for 24 h. (B) Images and quantification of A549 and H460 cell migration in Transwell migration chambers with 8-μm pores and stained with 0.1% crystal violet (×100). (C) A549 and H460 cells were administered MBZ (0.1 μM) for 48 h, and E-cadherin and N-cadherin expression was analyzed with western blotting. The independent assays were repeated three times. Relative to 0 μM of MBZ: ***, P<0.001. MBZ, mebendazole.

of NSCLC cells was triggered by ROS production. We found that MBZ could induce ROS generation, which could be rescued by administration of NAC (10 mM), a ROS scavenger (*Figure 3C*). Furthermore, NAC reduced the MBZ-triggered apoptosis of NSCLC cells (*Figure 3A*), indicating that apoptosis stimulated by MBZ may be a result of ROS aggregation.

MBZ regulated EMT and apoptosis through affecting the ROS-mediated STAT3 signaling cascade in NSCLC cells

ROS can modulate a number of cell signaling pathways, including the JAK2–STAT3 pathway (19,20). STAT3 is a transcription factor, which serves a pivotal role in tumor cell proliferation and progression (21). Hence, we aimed to

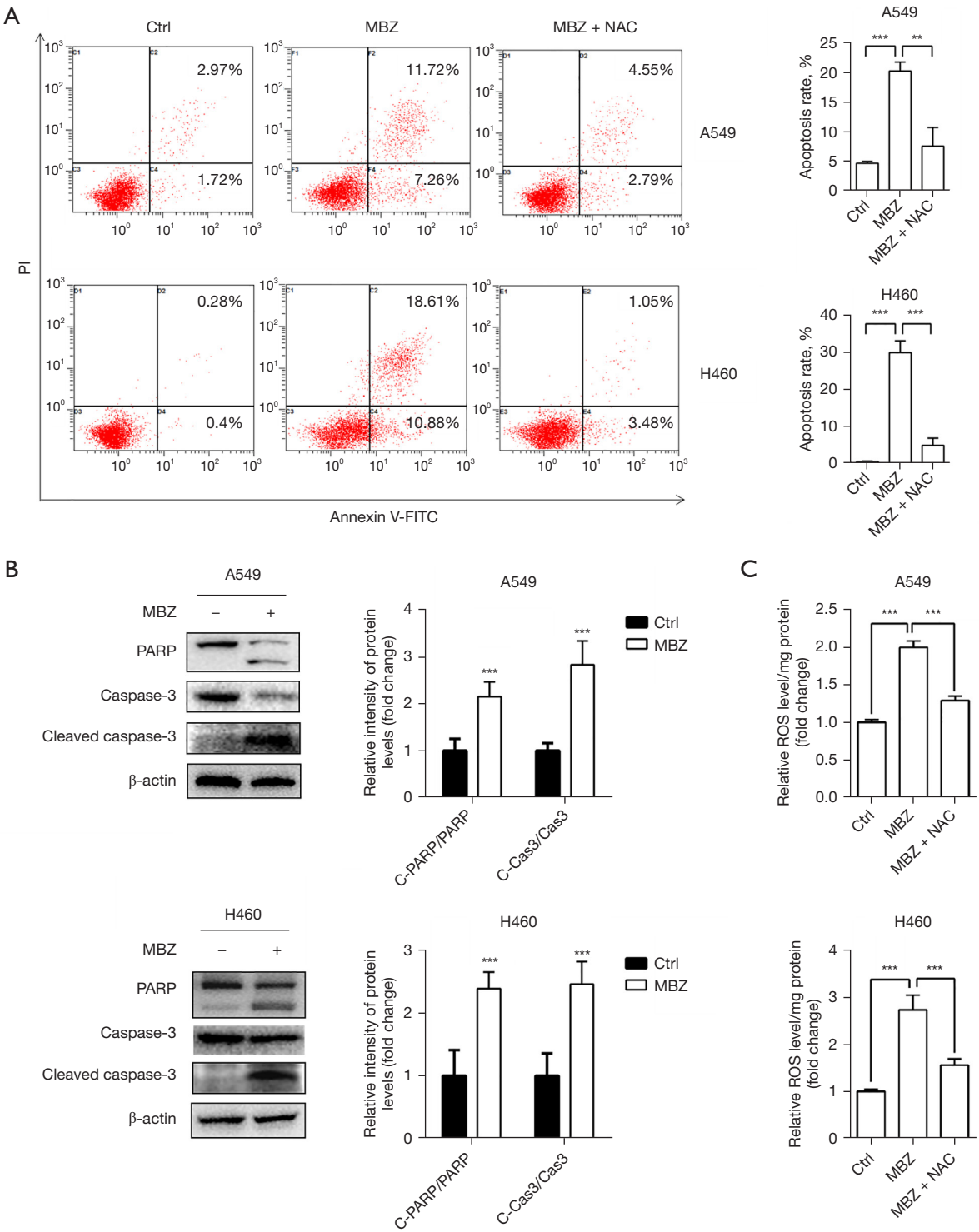

Figure 3 MBZ triggered apoptosis via ROS formation. (A) A549 and H460 cells were administered MBZ (0.5 μM) alone or in combination with NAC (10 mM) for 48 h, and apoptosis was assayed via flow cytometry. (B) A549 and H460 cells were administered MBZ (0.5 μM) for 48 h, and the expression of caspase-3, PARP, and cleaved caspase-3 were analyzed via Western blotting. (C) The level of ROS was detected in A549 and H460 cells with or without administration of MBZ (0.5 μM) and NAC (10 mM) with a multifunctional microplate reader. The independent assays were completed three times. **, P<0.01; ***, P<0.001. MBZ, mebendazole; NAC, N-acetylcysteine; FITC, fluorescein isothiocyanate; PI, propidium iodide; PARP, poly(ADP-ribose) polymerase; ROS, reactive oxygen species.

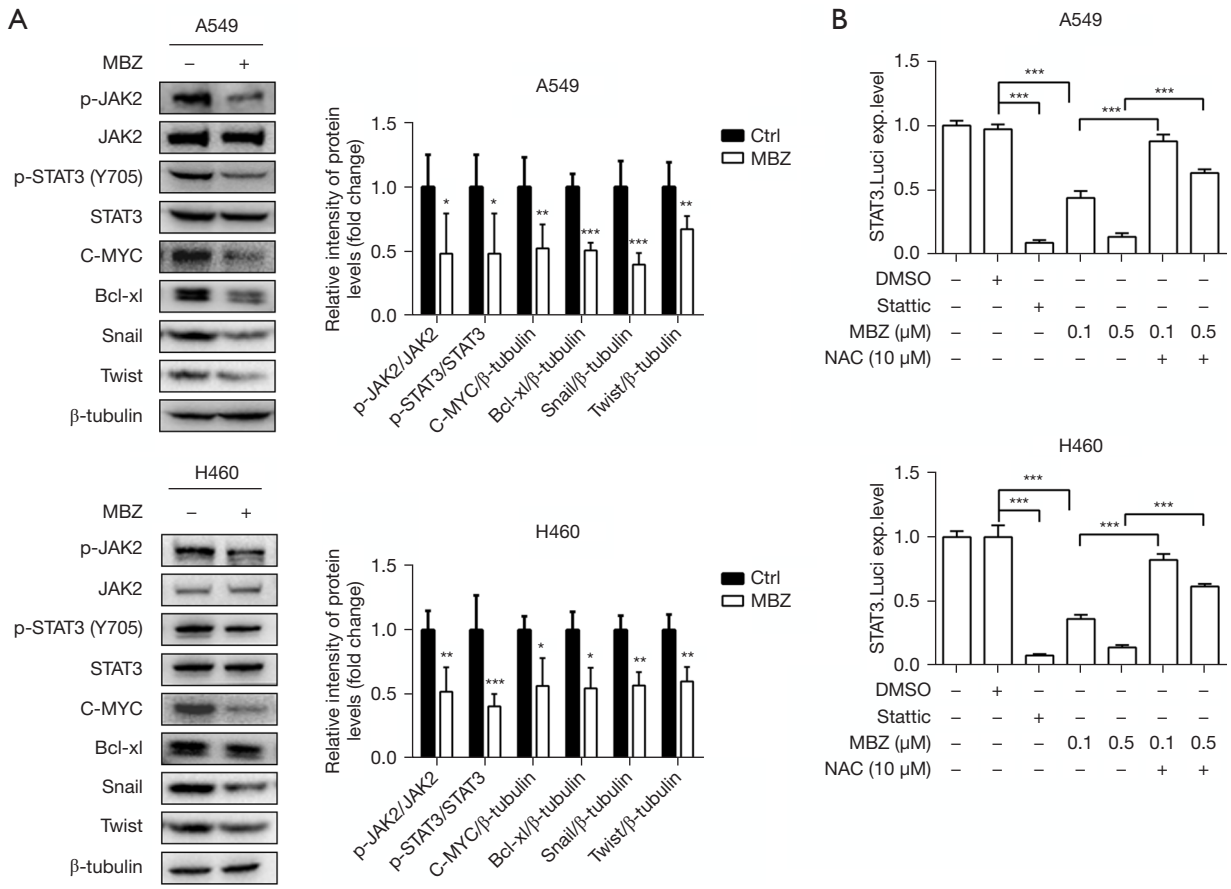

Figure 4 MBZ inhibited the ROS-JAK2-STAT3 signaling cascade in A549 and H460 cells. (A) The protein levels of JAK2-STAT3 signaling cascade treated with MBZ (0.5 μM) were investigated with Western blotting in A549 and H460 cells. (B) STAT3 Luci and β-gal plasmids were cotransfected into A549 and H460 cells. The cells were then administered MBZ alone or in combination with NAC for 48 h, which was followed by luciferase assays. Data from three independent assays were pooled. *, P<0.05; **, P<0.01; ***, P<0.001. MBZ, mebendazole; ROS, reactive oxygen species; JAK2, Janus kinase 2; STAT3, signal transducer and activator of the transcription 3; NAC, N-acetylcysteine.

determine whether MBZ can influence the JAK2–STAT3 signaling axis in NSCLC cells. Our findings demonstrated that p-JAK2 and p-STAT3 were suppressed in MBZ-treated cells, while total JAK2 and STAT3 did not change (*Figure 4A*). Additionally, the primary downstream targets of STAT3, including the antiapoptotic proteins, Bcl-xl and C-MYC, as well as the modulators of EMT, SNAI1 and TWIST1, were also inhibited by MBZ (*Figure 4A*). These findings thus confirmed MBZ's ability to affect EMT and apoptosis via targeting the STAT3 pathway.

Next, we explored whether MBZ affects the JAK2–STAT3 signaling cascade via ROS production in NSCLC cells. We measured the luciferase activity of STAT3 after treatment with or without MBZ and NAC for 48 h. Stattic, an inhibitor of STAT3 pathway, was used as a positive control. Our results showed that MBZ inhibited the STAT3 luciferase activity in a dose-dependent manner, and NAC could block the inhibition of STAT3 induced by MBZ (*Figure 4B*). Collectively, these results indicated that MBZ suppressed the JAK2-STAT3 signaling cascade via ROS generation in NSCLC cells.

MBZ suppressed NSCLC tumor growth in vivo

To investigate the therapeutic potential of MBZ for NSCLC *in vivo*, we established a xenograft model via the implantation of A549 cells. The tumor-bearing mice were divided into two groups (five mice per group) and orally administrated vehicle

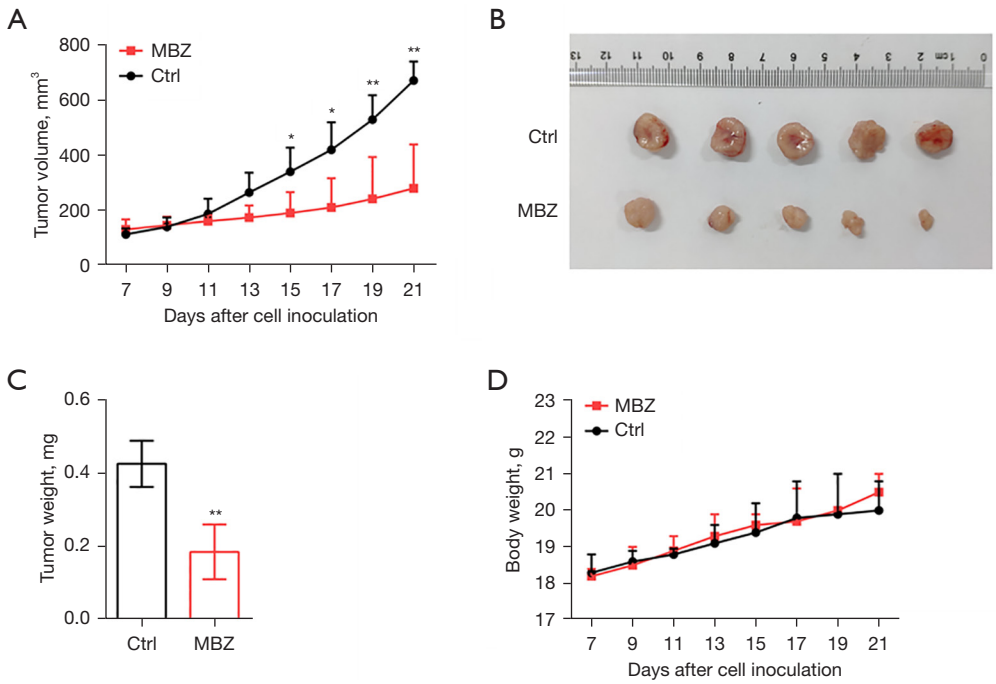

Figure 5 MBZ suppressed NSCLC tumor growth *in vivo*. Nude mice with human A549 subcutaneous tumor xenografts were established and treated with vehicle control and MBZ (50 mg/kg) every other day. (A) Tumor size was monitored every other day using a sliding caliper. After excision from the mice, the tumors were photographed (B) and weighed (C). (D) The body weight of the mice was measured every other day. *, P<0.05; **, P<0.01. MBZ, mebendazole; NSCLC, non-small cell lung cancer.

or MBZ (50 mg/kg). The tumor volume and weight were inhibited by MBZ (*Figure 5A-5C*). However, the body weight of mice demonstrated no significant differences between the two groups (*Figure 5D*), suggesting a satisfactory degree of safety in MBZ-treated mice.

Discussion

STAT3 activation is frequently observed in samples from NSCLC patients (22), and high p-STAT3 protein levels are associated with advanced disease stage, smoking, and epidermal growth factor receptor (EGFR)-mutation status (23). Furthermore, STAT3 inhibition impairs their survival in NSCLC cell lines and performs an essential function in promoting tumor-enhancing inflammation and evasion from antitumor immunity (24,25). Additionally, STAT3 can promote cancer hallmarks, including cell proliferation, migration, and anti-apoptosis by modulating the EMT process and the expression of oncogenes such as C-MYC, Survivin, BCL-xl, and hypoxia-inducible factor 1α (HIF-1α) (25,26). JAK/STAT3 signaling pathway is one of the important signal transduction pathways in cells. It has been reported that the JAK-STAT3 pathway is required for EMT in lung cancers (27), and activated STAT3 can promote EMT through the induction of Snail and Twist expression in cancers. Snail can repress the levels of E-cadherin, while the expression of N-cadherin is dependent on the expression of Twist (28). However, the mechanism of JAK-STAT3 in MBZ is still unclear. In this study, we found that MBZ could inhibit STAT3 activity as well as the expression of Snail and Twist, indicating a mechanism of inhibitory effect on cell migration. Consequently, targeting STAT3 directly or inhibiting upstream regulators may be a viable treatment strategy for the mitigation of NSCLC.

ROS is one of the most important regulators of apoptosis, and ROS generation activates the STAT3 pathway, resulting in tumor cell proliferation. In the normal physiological metabolism of tumors, the antioxidant systems can regulate the elevated ROS to maintain tumor cell survival (29). Antitumor drugs, such as cisplatin and docetaxel, often break the stability of oxidant and antioxidant systems (30,31). As a result, ROS production is able to silence some signaling cascades; for instance,

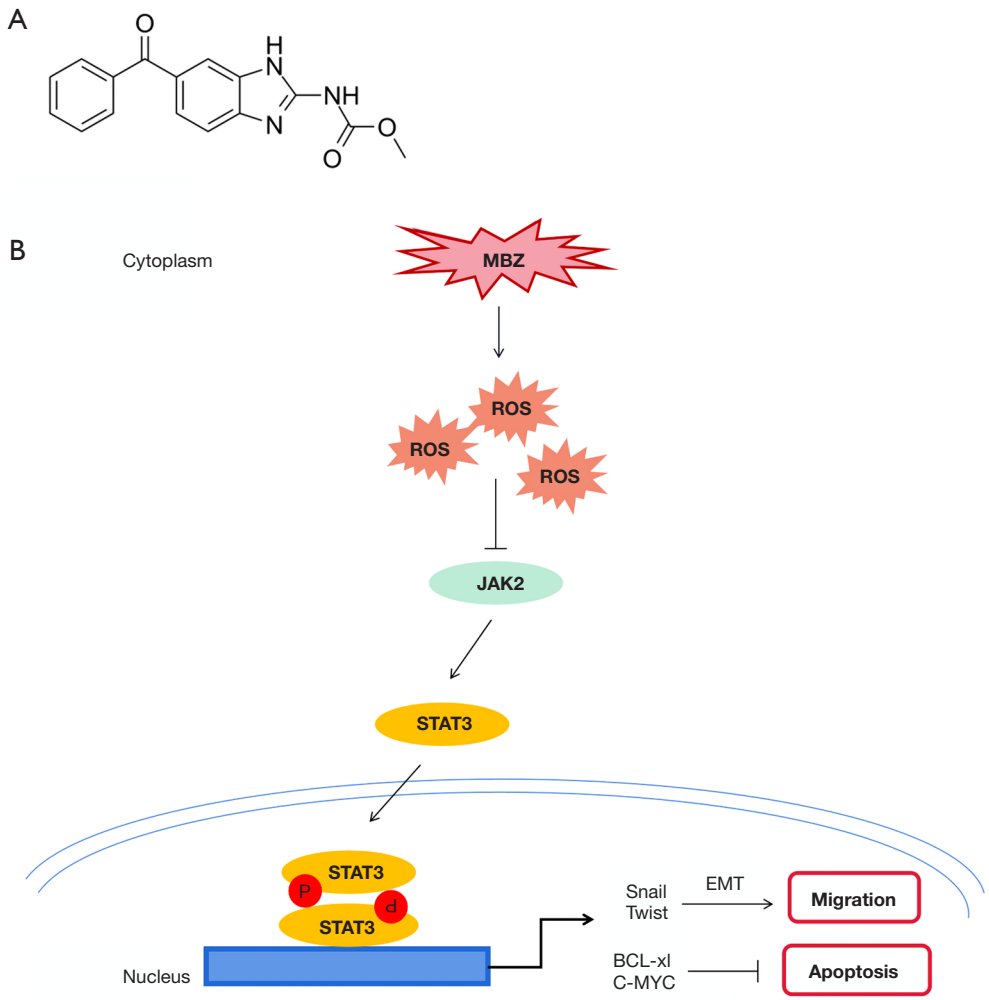

Figure 6 Proposed model of MBZ in regulating migration and apoptosis in NSCLC cells. (A) Chemical structure of MBZ. (B) Graphic demonstrating the action of MBZ in regulating migration and apoptosis in an NSCLC model. MBZ-induced ROS accumulation inhibits the JAK-STAT3 signaling pathway and the downstream genes including, *BCL-xl*, *C-MYC*, *SNAI1*, and *TWIST1*, resulting in the inhibitory effect on cell migration and the initiation of cell apoptosis. MBZ, mebendazole; ROS, reactive oxygen species; JAK, Janus kinase; STAT3, signal transducer and activator of the transcription 3; NSCLC, non-small cell lung cancer; BCL-xl, Bcl-2-like protein 1; C-MYC, Myc proto-oncogene protein; SNAI1, Zinc finger protein SNAI1; TWIST1, Twist-related protein 1.

the AKT-mTOR signaling axis (32) and the JAK-STAT3 signaling cascade (33), resulting in tumor cell apoptosis. We therefore hypothesized that MBZ-induced apoptosis is also the result of ROS generation in NSCLC cells, and we found that MBZ could induce ROS generation in A549 and H460 cells.

To our knowledge, this is the first study to demonstrate that MBZ can inhibit proliferation and migration by inducing cell apoptosis in NSCLC cells. Furthermore, MBZ suppressed NSCLC tumor growth *in vivo*. To examine the mechanism of MBZ activity, MBZ was used to treat the A549 and H460 cells, and the molecular expressions were determined using Western blotting. Our findings indicated that MBZ treatment caused a decreased expression level of p-JAK2 and p-STAT3, as well as that of downstream genes *BCL-xl*, *C-MYC*, *SNAI1*, and *TWIST1*, suggesting that MBZ inactivates the JAK2-STAT3 signaling pathway. Furthermore, MBZ treatment induced ROS generation, and the STAT3 activation and MBZ-induced apoptosis were rescued by NAC, a ROS scavenger. Therefore, ROS exerts a core role in MBZ-triggered NSCLC cell apoptosis via abrogating the JAK2-STAT3 signaling (*Figure 6A*,*6B*).

Conclusions

This study found that MBZ displays potent anti-NSCLC activity in both *in vitro* and *in vivo* models. Moreover, we identified that MBZ induces apoptosis and inhibits migration via ROS regulation of the STAT3 signaling pathway. Our findings may serve as the foundation for a novel strategy in NSCLC treatment.

Acknowledgments

Funding: This work was supported by the Science and Technology Development Foundation of Nanjing Medical University (No. NMUB20220186).

Footnote

Reporting Checklist: The authors have completed the ARRIVE and MDAR reporting checklists. Available at https://jtd.amegroups.com/article/view/10.21037/jtd-23-1978/rc

Data Sharing Statement: Available at https://jtd.amegroups.com/article/view/10.21037/jtd-23-1978/dss

Peer Review File: Available at https://jtd.amegroups.com/article/view/10.21037/jtd-23-1978/prf

Conflicts of Interest: All authors have completed the ICMJE uniform disclosure form (available at https://jtd.amegroups.com/article/view/10.21037/jtd-23-1978/coif). The authors have no conflicts of interest to declare.

Ethical Statement: The authors are accountable for all aspects of the work in ensuring that questions related to the accuracy or integrity of any part of the work are appropriately investigated and resolved. Animal experiments were performed under a project license (No. 202008A629) granted by ethics board of Soochow University, in compliance with institutional guidelines for the care and use of animals.

References

1. Siegel RL, Miller KD, Fuchs HE, et al. Cancer Statistics, 2021. CA Cancer J Clin 2021;71:7-33.
2. Yang SR, Schultheis AM, Yu H, et al. Precision medicine in non-small cell lung cancer: Current applications and future directions. Semin Cancer Biol 2022;84:184-98.
3. Chaudhary KR, Kinslow CJ, Cheng H, et al. Smurf2 inhibition enhances chemotherapy and radiation sensitivity in non-small-cell lung cancer. Sci Rep 2022;12:10140.
4. Zhang R, Meng Z, Wu X, et al. PD-L1/p-STAT3 promotes the progression of NSCLC cells by regulating TAM polarization. J Cell Mol Med 2022;26:5872-86.
5. Jiang H, Li X, Wang W, et al. MYCL promotes the progression of triple-negative breast cancer by activating the JAK/STAT3 pathway. Oncol Rep 2022;48:203.
6. Jia Y, Wang Q, Liang M, et al. KPNA2 promotes angiogenesis by regulating STAT3 phosphorylation. J Transl Med 2022;20:627.
7. Zhao Z, Wang Y, Gong Y, et al. Celastrol elicits antitumor effects by inhibiting the STAT3 pathway through ROS accumulation in non-small cell lung cancer. J Transl Med 2022;20:525.
8. Harris IS, DeNicola GM. The Complex Interplay between Antioxidants and ROS in Cancer. Trends Cell Biol 2020;30:440-51.
9. Wu Q, Li L, Miao C, et al. Osteopontin promotes hepatocellular carcinoma progression through inducing JAK2/STAT3/NOX1-mediated ROS production. Cell Death Dis 2022;13:341.
10. Zhu S, Xing C, Zhang G, et al. Icaritin induces cellular senescence by accumulating the ROS production and regulation of the Jak2/Stat3/p21 pathway in imatinib-resistant, chronic myeloid leukemia cells. Am J Transl Res 2021;13:8860-72.
11. Zhong Y, Le F, Cheng J, et al. Triptolide inhibits JAK2/STAT3 signaling and induces lethal autophagy through ROS generation in cisplatin-resistant SKOV3/DDP ovarian cancer cells. Oncol Rep 2021;45:69.
12. Xu WT, Shen GN, Li TZ, et al. Isoorientin induces the apoptosis and cell cycle arrest of A549 human lung cancer cells via the ROS-regulated MAPK, STAT3 and NF-κB signaling pathways. Int J Oncol 2020;57:550-61.
13. Choi HS, Ko YS, Jin H, et al. Mebendazole Increases

Anticancer Activity of Radiotherapy in Radiotherapy-Resistant Triple-Negative Breast Cancer Cells by Enhancing Natural Killer Cell-Mediated Cytotoxicity. Int J Mol Sci 2022;23:15493.
14. Son DS, Lee ES, Adunyah SE. The Antitumor Potentials of Benzimidazole Anthelmintics as Repurposing Drugs. Immune Netw 2020;20:e29.
15. Meco D, Attinà G, Mastrangelo S, et al. Emerging Perspectives on the Antiparasitic Mebendazole as a Repurposed Drug for the Treatment of Brain Cancers. Int J Mol Sci 2023;24:1334.
16. Kang B, Zhang X, Wang W, et al. The Novel IGF-1R Inhibitor PB-020 Acts Synergistically with Anti-PD-1 and Mebendazole against Colorectal Cancer. Cancers (Basel) 2022;14:5747.
17. Williamson T, Mendes TB, Joe N, et al. Mebendazole inhibits tumor growth and prevents lung metastasis in models of advanced thyroid cancer. Endocr Relat Cancer 2020;27:123-36.
18. Younis M, Wu Y, Fang Q, et al. Synergistic therapeutic antitumor effect of PD-1 blockade cellular vesicles in combination with Iguratimod and Rhodium nanoparticles. J Colloid Interface Sci 2023;649:929-42.
19. Fan S, He J, Yang Y, et al. Intermedin Reduces Oxidative Stress and Apoptosis in Ventilator-Induced Lung Injury via JAK2/STAT3. Front Pharmacol 2021;12:817874.
20. Li S, Wang H, Zhou Y. JAK2/STAT3 pathway mediates beneficial effects of pterostilbene on cardiac contractile and electrical function in the setting of myocardial reperfusion injury. Physiol Res 2022;71:489-99.
21. Dong Y, Chen J, Chen Y, et al. Targeting the STAT3 oncogenic pathway: Cancer immunotherapy and drug repurposing. Biomed Pharmacother 2023;167:115513.
22. Parakh S, Ernst M, Poh AR. Multicellular Effects of STAT3 in Non-small Cell Lung Cancer: Mechanistic Insights and Therapeutic Opportunities. Cancers (Basel) 2021;13:6228.
23. Han Y, Zhang Y, Tian Y, et al. The Interaction of the IFNγ/JAK/STAT1 and JAK/STAT3 Signalling Pathways in EGFR-Mutated Lung Adenocarcinoma Cells. J Oncol 2022;2022:9016296.
24. Kadariya Y, Sementino E, Shrestha U, et al. Inflammation as a chemoprevention target in asbestos-induced malignant mesothelioma. Carcinogenesis 2022;43:1137-48.
25. Guo Y, Mao W, Jin L, et al. Flavonoid Group of Smilax glabra Roxb. Regulates the Anti-Tumor Immune Response Through the STAT3/HIF-1 Signaling Pathway. Front Pharmacol 2022;13:918975.
26. Lin W, Sun J, Sadahira T, et al. Discovery and Validation of Nitroxoline as a Novel STAT3 Inhibitor in Drug-resistant Urothelial Bladder Cancer. Int J Biol Sci 2021;17:3255-67.
27. Wang LN, Zhang ZT, Wang L, et al. TGF-β1/SH2B3 axis regulates anoikis resistance and EMT of lung cancer cells by modulating JAK2/STAT3 and SHP2/Grb2 signaling pathways. Cell Death Dis 2022;13:472.
28. Lee JH, Mohan CD, Deivasigamani A, et al. Brusatol suppresses STAT3-driven metastasis by downregulating epithelial-mesenchymal transition in hepatocellular carcinoma. J Adv Res 2020;26:83-94.
29. Kirtonia A, Sethi G, Garg M. The multifaceted role of reactive oxygen species in tumorigenesis. Cell Mol Life Sci 2020;77:4459-83.
30. Swetha KL, Sharma S, Chowdhury R, et al. Disulfiram potentiates docetaxel cytotoxicity in breast cancer cells through enhanced ROS and autophagy. Pharmacol Rep 2020;72:1749-65.
31. Lin Z, Pan J, Chen L, et al. MiR-140 Resensitizes Cisplatin-Resistant NSCLC Cells to Cisplatin Treatment Through the SIRT1/ROS/JNK Pathway. Onco Targets Ther 2020;13:8149-60.
32. Fang S, Wan X, Zou X, et al. Arsenic trioxide induces macrophage autophagy and atheroprotection by regulating ROS-dependent TFEB nuclear translocation and AKT/mTOR pathway. Cell Death Dis 2021;12:88.
33. Chen B, Jia Y, Lu D, et al. Acute glucose fluctuation promotes in vitro intestinal epithelial cell apoptosis and inflammation via the NOX4/ROS/JAK/STAT3 signaling pathway. Exp Ther Med 2021;22:688.

Cite this article as: Liang Z, Chen Q, Pan L, She X, Chen T. Mebendazole induces apoptosis and inhibits migration via the reactive oxygen species-mediated STAT3 signaling downregulation in non-small cell lung cancer. J Thorac Dis 2024;16(2):1412-1423. doi: 10.21037/jtd-23-1978